Energetics, relative stabilities, and size-dependent properties of nanosized carbon clusters of different families: Fullerenes, bucky-diamond, icosahedral, and bulk-truncated structures

M. Yu,[a] I. Chaudhuri, C. Leahy, S. Y. Wu, and C. S. Jayanthi
Department of Physics, University of Louisville, Louisville, Kentucky 40292, USA

Structures and relative stabilities of carbon clusters belonging to different families have been investigated for diameters $d \leq 5$ nm based on an efficient semiempirical molecular dynamics (MD) scheme as well as a density functional theory based simulation. Carbon clusters studied include fullerenes and fullerene-derived structures (e.g., cages and onions), icosahedral structures, bucky-diamond structures, and clusters cut from the bulk diamond with spherical and facetted truncations. The reason for using a semiempirical MD is partly due to the large number of different cases (or carbon allotropes) investigated and partly due to the size of the clusters investigated in this work. The particular flavor of the semiempirical MD scheme is based on a self-consistent and environment-dependent Hamiltonian developed in the framework of linear combination of atomic orbitals. We find that (i) among the families of carbon clusters investigated, fullerene structures have the lowest energy with the relative energy ordering being $E_{\text{fullerene}} < E_{\text{onion}} < E_{\text{icosahedral}} < E_{\text{bucky-diamond}} < E_{\text{bulk-truncated}}$, (ii) a crossover between bucky-diamond and icosahedral structures is likely at $d \sim 8$ nm, (iii) the highest occupied molecular orbital-lowest unoccupied molecular orbital gap as a function of the diameter for the case of fullerenes shows an oscillatory behavior with the gap ranging from 2 eV to 6 meV, and the gap approaching that of gapless graphite for $d > 3.5$ nm, and (iv) there can be three types of phase transformations depending on the manner of heating and cooling in our simulated annealing studies: (a) a bucky-diamond structure $\rightarrow$ an onionlike structure, (b) an onionlike $\rightarrow$ a cage structure, and (c) a bucky-diamond $\rightarrow$ a cage structure. © *2009 American Institute of Physics.*
[DOI: 10.1063/1.3124827]

I. INTRODUCTION

Since the discovery of C_{60},[1] larger icosahedral fullerene structures,[2–7] structures with tetrahedral bonding and icosahedral symmetry ("diamond analogs of fullerenes"),[8] nested fullerenes ("onions")[9,10] with neighboring shells bound by van der Waals forces, and bucky-diamond structures[11] with tetrahedral bonding in the interior and sp^2-bonding on the exterior have been either synthesized, modeled, or discovered through computer simulation studies. The structural variety and richness exhibited by carbon clusters may be attributed to different types of bonding, corresponding to sp, sp^2, and sp^3 hybridizations between carbon atoms in an aggregate. On the other hand, other tetravalent elements such as silicon or germanium prefer to form exclusively sp^3 bonding, and hence the equilibrium structure of an aggregate of atoms in such elements is expected to have a tetrahedral network in the interior region and a reconstruction on the exterior region, which for a large cluster (i.e., a quantum dot or a nanoparticle) would resemble a bulk-truncated diamond structure with a reconstructed surface. But, a recent work by Zhao *et al.*[12] based on the density functional theory (DFT) revealed icosahedral structures to have lower energies compared to the bulk-truncated diamond structures in the case of silicon

clusters for diameters (d) less than 5 nm. However, for $d > 5$ nm, the bulk-truncated quantum dots were found to have lower energies.

Based on previous studies on carbon-based[8,11] and silicon-based nanostructures,[12,13] it is apparent that the structure and properties of low-dimensional systems are dictated by a combination of factors: size, surface characteristics (passivated versus unpassivated), bonding, and quantum confinement effects. In fact, the interplay among these factors is expected to be even more interesting in the case of carbon because of its diverse bonding characteristics. Specifically, these factors should play key roles in determining the relative stabilities of different families of carbon clusters, namely, the recently discovered bucky-diamond structures, icosahedral carbon structures (similar to those found in silicon), bulk-truncated structures, fullerenes, onions, and cage structures.

Barnard *et al.*[14] studied the relative stabilities of carbon nanoclusters belonging to different families using a model based on the atomic heat of formation. They have demonstrated that depending on the cluster size, bucky-diamond structures may coexist with fullerenes (~ 1.4 nm $< d < \sim 1.7$ nm), carbon onions (~ 1.4 nm $< d < \sim 1.7$ nm), or nanodiamond (~ 2.0 nm $< d < \sim 2.2$ nm).

A wide variety of theoretical methods ranging from *ab initio* methods,[5–7,11] tight-binding schemes,[4,15] to classical

---

a)Electronic mail: m0yu0001@gwise.louisville.edu.

potentials[8] has been employed to investigate the structure and electronic properties of carbon clusters of different sizes. An investigation of larger carbon clusters ($N > 500$) usually requires the use of linear scaling algorithms and the use of semiempirical quantum mechanical simulations. Despite the large number of theoretical studies devoted to the structural determination of carbon clusters, a consensus on the relative stability of different families of carbon clusters is lacking because these results were obtained from different methods with varying degrees of approximations. Therefore, it is desirable to perform simulations using the same computational approach (of an *ab initio* caliber) so that a quantitative comparison of energetics of different structures is possible.

The goal of the present work is to carry out a systematic study of the energetics of various known families of carbon clusters (C_N) up to relatively large sizes ($d \le 5$ nm) using the same highly efficient and reliable quantum mechanical simulation based on a recently developed self-consistent (SC) and environment-dependent (ED) Hamiltonian[16] implemented in the framework of linear combination of atomic orbitals (LCAOs). The diameter regime covered in the present paper goes beyond the regimes studied in Refs. 4, 5, 7, and 11. The carbon cluster families considered include fullerenes, icosahedral structures, cage structures (other than fullerenes), and different types of truncations of the bulk diamond (spherical and facetted truncations). In the case of bulk-truncated diamond clusters, the largest system investigated contains ~11 603 atoms, where we employ the linear scaling algorithm developed in Ref. 17. To validate the results obtained by the self-consistent and environment-dependent (SCED)-LCAO molecular dynamics (MD), we have also provided comparisons of our results with the DFT based simulations using the Vienna *ab initio* simulation package (VASP) (Ref. 18) for smaller diameter clusters, which was also performed in the present work. In this work, we will also verify the scenario reported in Ref. 14 for the coexistence of bucky-diamond structures with carbon onions and fullerenelike structures as well as the stability of icosahedral structures for carbon particles.

Although the general framework of the SCED-LCAO Hamiltonian is described in detail elsewhere,[16] we outline the essential features of this Hamiltonian in Sec. II so that the optimized SCED-LCAO parameters for carbon, as developed in this work, can be understood. The results corresponding to the energetics of different families of carbon clusters for different diameters and the phase transformation of bucky-diamond structures to onion and cage structures are elucidated in Sec. III.

II. SCED-LCAO HAMILTONIAN AND OPTIMIZED CARBON PARAMETERS

The basic premise of the SCED-LCAO method is to go beyond the traditional two-center tight-binding Hamiltonians[19] by including ED electron-ion and electron-electron interactions and the SC treatment of charge redistributions. The total energy using the SCED-LCAO Hamiltonian is given by the following expression:

$$E_{tot} = E_{BS} + \frac{1}{2}\sum_i (Z_i^2 - N_i^2)U_i - \frac{1}{2}\sum_{i,k(i \ne k)} N_i N_k V_N(R_{ik})$$
$$+ \frac{1}{2}\sum_{i,k(i \ne k)} Z_i Z_k V_C. \tag{1}$$

The first term in Eq. (1) represents the band structure energy (E_{BS}), the second and third terms represent corrections to the double counting of electron-electron interactions, and the last term is the repulsive interaction between ion cores. The band structure energy is obtained by solving the generalized eigenvalue equation $Hc_\lambda = E_\lambda S c_\lambda$, where $\underline{H}$ and S represent the Hamiltonian and overlap matrices and $E'_\lambda s$ and $C'_\lambda s$ are the eigenvalues and eigencoefficients. In the second term of Eq. (1), Z_i is the number of valence electrons associated with an isolated atom at site i, N_i is the number of electrons associated with the atom at site i when it is in the aggregate, and U_i is a parameter akin to the on-site Hubbard energy. The term $V_N(R_{ik})$ represents the electron-electron interaction energy per electron charge between the electron associated with the ion at site k and the electron associated with the ion at site i. In fact, $V_N(R_{ik})$ can be expressed in terms of $V_Z(R_{ik})$, the electron-ion interaction energy per ionic charge, and a short-range function $\Delta V_N(R_{ik})$ as $V_N(R_{ik}) = V_Z(R_{ik}) + \Delta V_N(R_{ik})$. This is possible because both $V_N(R_{ik})$ and $V_Z(R_{ik})$ approach $e^2/4\pi\varepsilon_0 R_{ik}$ as $R_{ik} \to \infty$. Finally, V_C in the fourth term of Eq. (1) is the Coulomb interaction potential per ionic charge with $V_C = E_0/R_{ik}$ ($E_0 = e^2/4\pi\varepsilon_0$).

The SCED-LCAO Hamiltonian matrix elements can be constructed using the expression

$$H_{i\alpha,j\beta}^{SCED\text{-}LCAO} = \frac{1}{2}\Bigg\{ K(R_{ij})(\varepsilon'_{i\alpha} + \varepsilon'_{j\beta}) + \Big[(N_i - Z_i)U_i + (N_j$$
$$- Z_j)U_j\Big] + \Bigg[\sum_{k \ne i}(N_k V_N(R_{ik}) - Z_k V_Z(R_{ik}))$$
$$+ \sum_{k \ne j}(N_k V_N(R_{jk}) - Z_k V_Z(R_{jk}))\Bigg]\Bigg\}S_{i\alpha,j\beta}(R_{ij}).$$
$$\tag{2a}$$

The first term in Eq. (2a) is the extended Hückel term; $\varepsilon'_{i\alpha}$ is related to the energy of an electron associated with an ion at site i in the orbital α; $K(R_{ij})$ represents a scaling function defined as $K(R_{ij}) = e^{\alpha_K R_{ij}}$. The functional forms chosen for $V_Z(R_{ik})$ and $\Delta V_N(R_{ik})$ are

$$V_Z(R_{ik}) = E_0\{1 - (1 + B_Z R_{ik})e^{-\alpha_Z R_{ik}}\}/R_{ik}, \tag{2b}$$

$$\Delta V_N(R_{ik}) = (A_N + B_N R_{ik})[1 + e^{-\alpha_N d_N}]/[1 + e^{-\alpha_N(d_N - R_{ik})}]. \tag{2c}$$

Finally, the overlap matrix element in Eq. (2a) is defined through the following expression:

$$S_{ij,\tau} = (A_\tau + B_\tau R_{ij})[1 + e^{-\alpha_\tau d_\tau}]/[1 + e^{-\alpha_\tau(d_\tau - R_{ij})}]. \tag{3}$$

In Eq. (3) τ denotes the molecular orbitals corresponding to a given basis set (e.g., τ corresponds to $ss\sigma$, $sp\sigma$, $pp\sigma$, and $pp\pi$ in a sp^3 basis set). A great deal of attention has been given in the choosing functional forms for $K(R_{ij})$, $V_Z(R_{ik})$, $\Delta V_N(R_{ik})$, and $S_{ij,\tau}$.

TABLE I. Optimized SCED-LCAO parameters for carbon.

ε_s (eV)	−17.360	$\alpha_{ss\sigma}$ (Å⁻¹)	2.153
ε_p (eV)	−8.329	$d_{ss\sigma}$ (Å)	0.629
ε_s' (eV)	−35.712	$B_{sp\sigma}$ (Å⁻¹)	−0.777
ε_p' (eV)	−22.153	$\alpha_{sp\sigma}$ (Å⁻¹)	2.013
α_K (Å⁻¹)	−0.0329	$d_{sp\sigma}$ (Å)	0.782
U (eV)	14.896	$B_{pp\sigma}$ (Å⁻¹)	−1.895
B_Z (Å⁻¹)	1.475	$\alpha_{pp\sigma}$ (Å⁻¹)	1.881
A_N (eV)	−2.539	$d_{pp\sigma}$ (Å)	0.377
B_N (Å⁻¹)	−1.798	$B_{pp\pi}$ (Å⁻¹)	0.236
α_N (Å⁻¹)	3.115	$\alpha_{pp\pi}$ (Å⁻¹)	2.255
d_N (Å)	0.800	$d_{pp\pi}$ (Å)	0.547
$B_{ss\sigma}$ (Å⁻¹)	0.228	R_{cut} (Å)	4.0

Practical applications based on the SCED-LCAO Hamiltonian requires, as a first step, the determination of parameters (ε_S', ε_P', α_K, U, B_Z, α_Z, A_N, B_N, α_N, d_N, A_τ, B_τ, α_τ, and d_τ) appearing in the Hamiltonian for the system under investigation. This is achieved by combining the Marquardt–Levenberg algorithm[20] for determining the local minimum of a least squares sum for the objective function with a global optimization scheme.[16] The objective function depends on the parameters of the model and is evaluated using the definition of the least squares sum of the difference between the calculated properties (SCED-LCAO) and the reference properties (*ab initio* results). The reference properties, as calculated from *ab initio* calculations, constitute the database of properties of our system. In the case of carbon, our database is comprised of bond lengths and binding energies of carbon clusters for $N \leq 6$ (calculated using the Gaussian package MPW1PW91/cc-ppVTZ) (Ref. 21) and bulk cohesive energies for a variety of phases[22] and the band structure for the diamond phase [calculated using the DFT-based VASP package[18] in the local density approximation (LDA)]. Corresponding to each one of the physical and chemical properties in the database, the same properties are also evaluated using the SCED-LCAO approach, and the parameters of the SCED-LCAO Hamiltonian are varied until the desired low residue is obtained for the objective function in our fitting algorithm. The optimized carbon parameters thus obtained for the SCED-LCAO method are summarized in Table I. In order to check the quality of the optimized parameter set for carbon, we have compared the *ab initio* results (for binding energies and bond lengths) obtained for small carbon clusters ($N \leq 6$) of different symmetries with those obtained from the SCED-LCAO method (see Table II). We have also deliberately included a few metastable clusters in the database so that our parameter set can represent all sorts of complex environments. The agreement between the SCED-LCAO and the *ab initio* results for bond lengths and binding energies is remarkable (see Table II). Figure 1 compares the bulk phase diagrams for diamond, graphite, simple cubic (sc), body-centered cubic (bcc), and face-centered cubic (fcc) as obtained by the DFT/LDA calculation[18] and the SCED-LCAO method using the optimized parameter set given in Table. I The quantity plotted in Fig. 1 is the relative energy versus the relative atomic volume (V/V_0), where the relative energy is defined as the total energy per atom of a bulk phase (graph-

TABLE II. Bond lengths (Å) and binding energies (eV) for carbon clusters ($N \leq 6$) in different configurations as obtained by the SCED-LCAO method (present work) and *ab initio* calculations (Ref. 21).

C_N	Symmetry	Present work	*Ab initio* values
C_2	D_{ih}	1.293 Å	1.244 Å
		−5.228 eV	−4.527 eV
C_3	D_{ih}	1.329 Å	1.287 Å
		−6.588 eV	−6.586 eV
C_3	C_{2v}	1.326 Å	1.256 Å
		1.515 Å	1.459 Å
		−5.988 eV	−6.225 eV
C_4	D_{2h}	1.488 Å	1.439 Å
		−6.698 eV	−6.746 eV
C_4	D_{ih}	1.324 Å	1.288 Å
		1.361 Å	1.306 Å
		−6.520 eV	−6.620 eV
C_4	D_{2d}	1.382 Å	1.316 Å
		1.554 Å	1.555 Å
		−5.631 eV	−5.566 eV
C_4	T_d	1.577 Å	1.621 Å
		−5.510 eV	−4.830 eV
C_5	D_{ih}	1.325 Å	1.277 Å
		1.341 Å	1.282 Å
		−7.124 eV	−7.319 eV
C_5	D_{3h}	1.487 Å	1.488 Å
		2.113 Å	2.013 Å
		−6.917 eV	−6.578 eV
C_5	C_{4v}	1.495 Å	1.443 Å
		1.607 Å	1.668 Å
		−6.547 eV	−6.242 eV
C_5	T_d	1.409 Å	1.417 Å
		2.301 Å	2.314 Å
		−5.521 eV	−5.100 eV
C_6	D_{3h}	1.909 Å	1.823 Å
		2.090 Å	1.864 Å
		−6.995 eV	−7.443 eV
C_6	D_{6h}	1.349 Å	1.298 Å
		−6.985 eV	−7.297 eV
C_6	D_{ih}	1.332 Å	1.270 Å
		1.329 Å	1.285 Å
		1.355 Å	1.294 Å
		−7.054 eV	−7.291 eV
C_6	D_{4h}	1.519 Å	1.536 Å
		1.824 Å	1.790 Å
		−6.909 eV	−6.467 eV
C_6	D_{5v}	1.406 Å	1.354 Å
		1.689 Å	1.698 Å
		−6.158 eV	−6.254 eV

ite, sc, bcc, fcc, etc.) minus the total energy per atom of the diamond phase at its equilibrium volume (V_0). The bulk relative energy results agree excellently with DFT calculations.[22]

To further test the viability of the parameter set for predictive simulations, we investigated the equilibrium structure of an intermediate size C_{147} cluster (see Fig. 3). The initial structure of this cluster was constructed from the spherical truncation of the bulk diamond structure. Upon relaxation of this structure, the bucky-diamond structure (i.e., a diamond-like core of 35 atoms connected to a fullerene shell of 112 atoms) emerged automatically as the relaxed stable structure, which was also found in a DFT-based simulation.[11] It should
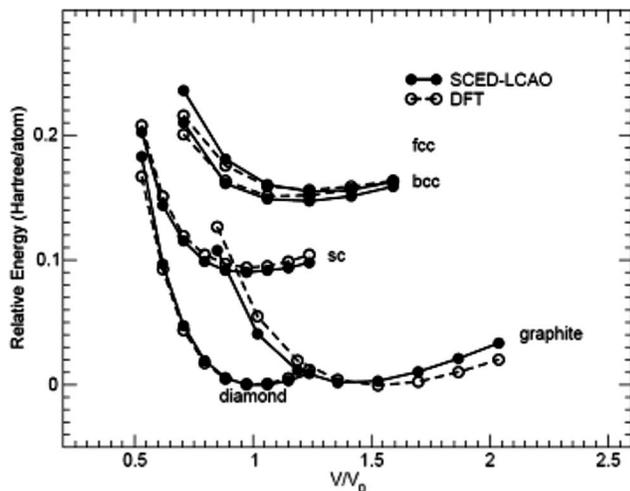
FIG. 1. A comparison of the results as obtained from the SCED-LCAO (solid curves) and DFT-LDA (Ref. 22) (dotted curves) calculations for the relative energy $(E-E_0)$ vs the relative atomic volume shown for different bulk phases of carbon (e.g., diamond, graphite, sc, bcc, and fcc structures), where E refers to the total energy per atom of any bulk phase and E_0 refers to that of the bulk diamond at its equilibrium volume (V_0).
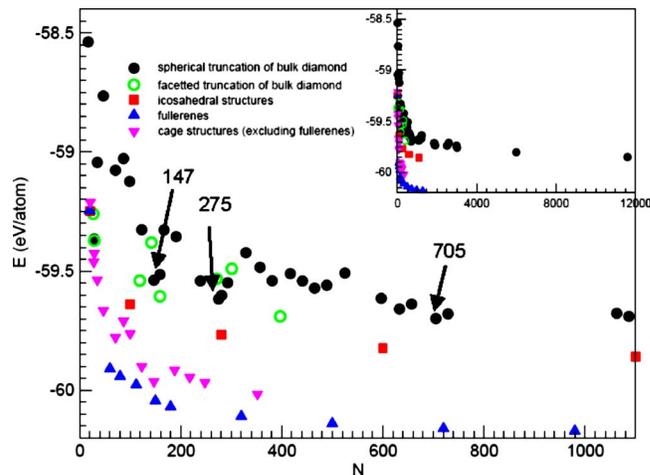

FIG. 2. (Color online) The total energy per atom E as a function of the number of atoms N in the cluster is shown for a variety of different carbon families starting from different initial structures: (i) spherical (filled circles) and facetted (open circles) truncations of the bulk diamond, (ii) icosahedral structures (filled squares), (iii) fullerenes (upright triangles), and (iv) cage structures excluding fullerenes (inverted triangles). The arrows indicate the local minima in the E vs N curve corresponding to the bucky-diamond structures (C_{147}, C_{275}, and C_{705}). The inset includes the results for larger bulk-truncated diamond clusters ($N>1000$) and it can be seen that even at $N=11\,603$, the energy/atom of the bulk-truncated cluster is 0.3 eV higher than that of the graphite ($E=-60.19$ eV), while this quantity for fullerenes has converged to that of the graphite at $N\sim1300$ atoms.

be mentioned that when we performed the same calculation using a two-center tight-binding Hamiltonian,[19] we were not able to get the bucky-diamond structure starting from the same initial C_{147} configuration.[23] The test performed on the C_{147} cluster, an intermediate sized carbon cluster, further confirms the transferability of the carbon parameters to an even more complex chemical environment, and it suggests that the SCED-LCAO Hamiltonian may be used for predictive material simulations of other low-dimensional carbon structures.

III. RESULTS AND DISCUSSIONS

A. Energetics and relative stabilities of different families of carbon clusters

In this section we investigate first the energetics of different families (or allotropes) of carbon clusters for diameters $d\leq5$ nm based on the total energy calculation of relaxed structures using the parameters given in Table I. Relaxations are performed using the SCED-LCAO MD in which the atomic forces, evaluated as Hellman–Feynman forces, are obtained from the energy expression given in Eq. (1). Specific initial structures considered include (i) bulk-terminated diamond structures (with spherical and facetted truncations), (ii) fullerenes (containing only pentagons and hexagons), (iii) cage structures or fullerenelike structures (containing other polygons in addition to hexagons and pentagons), (iv) icosahedral structures,[12] (v) onion structures,[10] etc. In the case of facetted bulk truncation, the initial configurations were constructed with no more than one dangling bond on surface atoms. Furthermore, for each family of carbon clusters, we considered initial configurations corresponding to different diameters with the size of the clusters up to about 5 nm. For bulk truncated diamond structures with spherical truncation, we have carried out the simulations up to $\sim11\,600$ atoms. For cluster sizes larger than 1500 atoms, we used the order-N scheme[17] to determine the equilibrium

structures. In our simulation, all of the initial configurations were relaxed until the force on each atom of a given system was less than ~0.01 eV/Å.

The total energy per atom (E) of various types of carbon clusters as a function of the total number of atoms N is shown in Figure 2 for N up to ~1100 atoms. First, we examine the total energy per atom for the clusters with spherical bulk truncation denoted by full circles in Fig. 2. It can be seen that in addition to the general trend of decreasing energy with respect to the total number of atoms, one can also identify some explicit local minima for the spherically truncated clusters. It turns out that some of these local minima correspond to bucky-diamond clusters (C_{147}, C_{275}, and C_{705}) (Ref. 11). This is really quite remarkable since it indicates that the relaxation scheme based on the SCED-LCAO Hamiltonian can lead directly from the initial configurations of spherical bulk truncation of tetrahedral networks to bucky-diamond structures at precisely $N=147$, 275, and 705, demonstrating the robustness of the SCED-LCAO Hamiltonian. To shed light on the existence of the local minima in Fig. 2, we have carried out a detailed structural analysis of the relaxed structures of clusters obtained from the spherical truncation of the bulk diamond. In particular, we have characterized the structure by the number of dangling bonds $(n_{dangling}^i)$ associated with each cluster in this family and the type of polygonal rings (three-member rings, four-member rings, etc.) on the surface of the cluster. We have used the four-atom coordination corresponding to the complete sp^3 bonding nature of a tetravalent atom as our definition for "no dangling bond" (i.e., $n_{dangling}^0$). Therefore, the term such as "no more than one dangling bond" refers to atoms in the carbon clusters having either three (one dangling bond:

TABLE III. Analysis of dangling bonds and the nature of the coordination for relaxed carbon structures (C_N) with spherical truncations of the bulk diamond, where N denotes the total number of atoms in the cluster and $n_{dangling}^i$ denotes the number of atoms with i dangling bonds. The word "yes" in columns 5 and 6 means that there are three-member rings or four-member rings in the corresponding cluster C_N.

C_N	$n_{dangling}^1$	$n_{dangling}^2$	$n_{dangling}^3$	Three-member rings	Four-member rings
C_{17}	12			Yes	
C_{29}	23			Yes	Yes
C_{35}	16	6		Yes	Yes
C_{47}	24	6		Yes	
C_{71}	30	5		Yes	Yes
C_{87}	34	13		Yes	Yes
C_{99}	33	15		Yes	Yes
C_{123}	56	12			
C_{147}	108				
C_{159}	100			Yes	
C_{167}	64	12	4		
C_{191}	55	10	1	Yes	Yes
C_{239}	55	9		Yes	Yes
C_{275}	144				
C_{281}	132	6		Yes	
C_{293}	120	6		Yes	
C_{329}	76	12		Yes	Yes
C_{357}	100	24		Yes	Yes
C_{381}	151	18		Yes	Yes
C_{417}	124	24		Yes	Yes
C_{441}	140	24		Yes	
C_{465}	164	12		Yes	
C_{489}	128	12		Yes	Yes
C_{525}	132	40			Yes
C_{597}	156	24			
C_{633}	208	22		Yes	
C_{657}	196	12			
C_{705}	276				
C_{729}	264			Yes	

$n_{dangling}^1$) or four nearest neighbors (no dangling bond: $n_{dangling}^0$). It is also known that the surface reconstruction of an ideal tetrahedral network leading to three-member or four-member rings represents some local distortions in the network of a cluster structure. The results of our analysis based on these criteria are summarized in Table III. It can be seen that while the local minima occur at $N=29$, 71, 147, 275, 381, 465, 633, and 705 (see Fig. 2), only those at $N=147$, 275, and 705 share two unique common properties: (i) these clusters do not have three-member and four-member rings on their surfaces and (ii) the atoms in these clusters have no more than one dangling bond.

Since carbon atoms can form either sp^2 bonds (with three nearest neighbors) or sp^3 bonds (with four nearest neighbors), a carbon cluster with its atoms having no more than one dangling bond is therefore a more stable cluster compared to a neighboring carbon cluster (i.e., $N_{j+1}=N_j\pm1$) with their component atoms having more than one dangling bond and/or having three-member/four-member rings, where N_j represents the size of the jth bucky-diamond cluster (i.e., $N_j=147$, 275, and 705). Hence, for the curve of the total energy per atom of spherically bulk truncated carbon clusters, the clusters with $N_j=147$, 275, or 705 are the local minima with respect to their neighbors. Furthermore, in the relaxed configuration of spherically truncated clusters with

no more than one dangling bond, those atoms having four nearest neighbors (with sp^3 bonding) will remain in the diamond structure while those atoms with three nearest neighbors (with sp^2 bonding) will form fullerenelike shell, leading to the bucky-diamond structure.

In Fig. 2, the total energies per atom of clusters of facetted bulk truncations and that of icosahedral clusters are also shown and denoted by open circles and solid squares, respectively. We found that the energy curve of the icosahedral structure exhibits a general smooth decreasing pattern, having lower energy per atom compared to the clusters with bulk truncated structures. To shed light on why carbon cluster with the icosahedral structure is more stable than bucky-diamond structure, we analyzed these structures further. In particular, we have provided a rationale based on the structural analysis of the bucky diamond C_{147}. This structure has 35 atoms in its interior and 112 atoms on the exterior. The interior atoms form a tetrahedral network with sp^3-type bonding, while the exterior atoms form fullerenelike shells with sp^2-type bonding (see Figs. 3 and 4). The fullerenelike outer shell is formed by four (111) surface facets connected by pentagons. The distance between the atoms in the inner core and the atoms in the outer shell lie in the range of 2.2 Å–2.6 Å. On the other hand, for an icosahedral carbon cluster, e.g., C_{100} (with its diameter comparable to bucky dia-
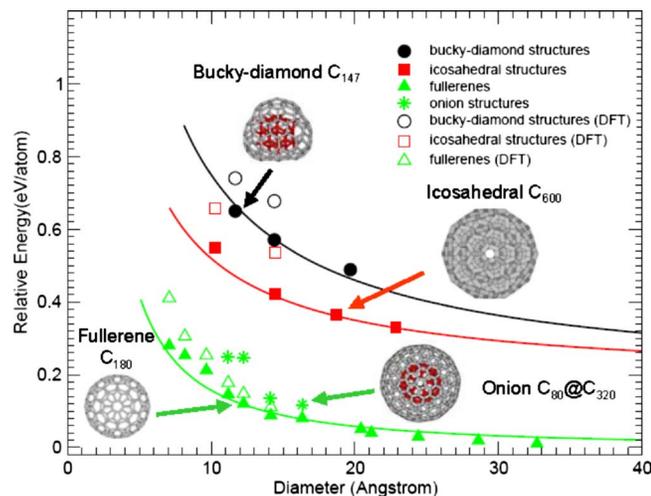
FIG. 3. (Color online) The results obtained for the diameter dependence of the relative energy (the total energy per atom of the cluster minus the total energy per atom of the graphite) using both the SCED-LCAO method (filled symbols) and the DFT-based *ab initio* simulation (open symbols) are shown for bucky diamonds (filled circles/open circles), icosahedral structures (filled squares/open squares), and fullerenes (filled triangles/open triangles). Knowing the number of atoms (N) in the cluster, the correspondence between the diameter (d) of the cluster and the number of atoms in the cluster can be readily calculated (see the main text). In the figure the results are shown for diameters corresponding to $N=100$, 280, 600, and 1100 in the case of icosahedral structures; $N=147$, 275, and 705 for bucky diamonds; and $N=60$, 80, 112, 150, 180, 240, 320, 500, 540, 720, 980, and 1280 for fullerenes. In the case of onion structures, the results are shown using the SCED-LCAO method only, and they have been calculated for four diameters corresponding to the structures $C_{20}@C_{150}$, $C_{60}@C_{180}$, $C_{60}@C_{240}$, and $C_{80}@C_{320}$.

mond C_{147}), the atomic separation between surface atoms and interior atoms adjacent to the surface is ~ 1.6 Å. The weak bonding between the inner core and the outer shell in a bucky-diamond structure renders this structure less stable
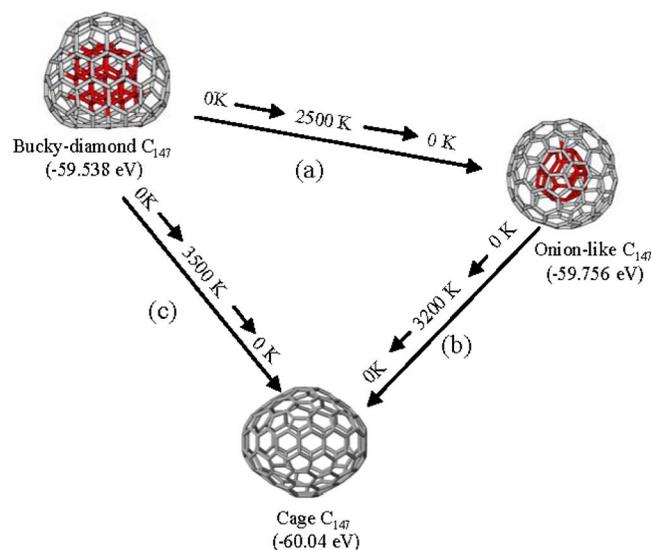

FIG. 4. (Color online) Phase transformations of a C_{147} cluster: (a) a bucky-diamond structure to an onion structure (heated to 2500 K and slowly cooled to 0 K); (b) an onion structure to a cage structure (heated to 3200 K and slowly cooled to 0 K); and (c) a bucky-diamond structure to a cage structure (heated to 3500 K and slowly cooled to 0 K). The total energy per atom for each phase is indicated in the parentheses.

compared to the icosahedral structure, despite the lowering of energy caused by the formation of a fullerenelike shell in a bucky-diamond structure.

The total energies per atom of cage structures (inverted triangles) and fullerenes (upright triangles) are also shown in Fig. 2. It can be seen that clusters of cage structures and fullerenes are more stable than the families of bulk truncated clusters and icosahedral clusters with fullerenes having the lowest energy. To further confirm that fullerene structures have the lowest energy among all families (or allotropes) of carbon clusters, we have extended our calculations for clusters with spherical bulk truncation up to the size of $\sim 11\,600$ atoms. The results are shown in the inset of Fig. 2 (filled circles with $N>1000$). It can be seen from the inset of Fig. 2 that the energy/atom of the fullerene structure has reached that of the graphite (~ -60.19 eV) for $N\sim 1300$, while the energy/atom of the bulk-truncated diamond cluster is ~ 0.3 eV/atom higher than that of graphite even at $N\sim 11\,600$, and the energy/atom of other carbon families falls within these two limits, confirming that fullerene structures have the lowest energy among all families of carbon clusters. Clearly, this result is different from the case of silicon[12] in which the icosahedral structures were found to have lower energies compared to clusters with bulk-terminated diamond structures for $d\leq 5$ nm. The fact that fullerene structures have the lowest energy compared to other carbon families can be simply attributed to the sp^2-bonded nature of carbon atoms in the shell. In a previous study, Zhang *et al.*[4] found that C_{60}, C_{70}, and C_{84} are energetically more stable due to their high fragmentation stability and chemical reactivity.

To complement the findings in Fig. 2 and to further delineate the results, we have studied the diameter dependence of the relative energy ($\varepsilon=E-E_g$), which is defined as the total energy per atom of the cluster (E) minus the total energy per atom of the graphite (E_g) for four of the families of carbon clusters: bucky-diamond structures, icosahedral structures, onions, and fullerenes. The diameters for bulk truncated and icosahedral clusters are calculated through the formula $4\pi(d/2)^3/3=Na_d^3/8$ and those for fullerenes, cages, and onions are calculated through the formula $4\pi(d/2)^2=Na_g^2\sin(\pi/3)/2$, where a_d and a_g refer to the lattice constants of the bulk diamond and the graphite, respectively. Based on these equations for the diameters, it is evident that for the same size (d) but different types of carbon clusters, the total number of atoms N is larger in bulk-truncated or icosahedral clusters than in cagelike clusters. This is one of the reasons for plotting the relative energies as a function of the diameter. Additionally, by fitting ε versus d to a functional form, characterizing the diameter dependence of the relative energies of different families, we should be able to predict the crossover diameters for the relative stabilities of different carbon families.

In Fig. 3, the relative energy (ε) versus d curve exhibits a monotonic decrease as d increases for all families of carbon clusters, and this behavior can be fitted to the formula $\varepsilon=\varepsilon_0+\alpha/d^\beta$ with the coefficients ε_0, α, and β having different values for different structures. In particular, $\varepsilon_0=0.20$ eV/atom, $\alpha=5.8$ eV Å/atom, $\beta=1$ for the bucky-diamond structure; $\varepsilon_0=0.23$ eV/atom, $\alpha=3.4$ eV Å/atom,

$\beta=1$ for the icosahedral structure; and $\varepsilon_0=0$, $\alpha=4.0$ eV Å$^{1.4}$/atom, $\beta=1.4$ for fullerenes. Other features exhibited in Fig. 3 are the following. (i) ε versus d curves for both bucky-diamond and icosahedral structures have their relative energies higher than that of the bulk diamond structure even as $d\rightarrow\infty$. (ii) On the other hand, the relative energy of the fullerenes approaches zero for $d\sim 4$ nm. The results for ε versus d curves for the bucky-diamond and the icosahedral families suggest a possible crossover between these two structures for $d>4$ nm. Using the diameter-dependence formula for the relative energy corresponding to bucky-diamond and icosahedral families, we estimate the crossover between these two structures to occur at $d\sim 8$ nm. We recognize that the estimated crossover diameter may not be very accurate because of the very few data points used in the fitting, but a crossover between the two structures beyond 4 nm must exist simply because the relative energy per atom of the bucky-diamond structures at large enough diameters is expected to approach that of the bulk diamond while the icosahedral structure is expected to be unstable with respect to the diamond phase as $d\rightarrow\infty$ (icosahedral symmetry being incompatible with the full bulk symmetry). In fact, a similar crossover behavior between icosahedral clusters and bulk truncated clusters has already been reported for silicon.[12] On the other hand, there is no indication of a crossover between the relative energy versus diameter curve of the fullerene family and that for the rest of the carbon family clusters.

Based on our diameter-dependent energetic studies (Fig. 3), onions have lower energies compared to bucky-diamond structures and there is no crossover between the curves for relative energy versus diameter corresponding to the bucky-diamond and onion structures for $d\leq 4$ nm. Our results, therefore, do not support the coexistence of onion and bucky-diamond structures, as reported in Ref. 14, for diameters in the regime ~ 1.7 nm $<d<\sim 2.0$ nm. Similarly, our calculations do not support the coexistence of bucky diamond and fullerenes as predicted in Ref. 14.

In Fig. 3, we have also included the results of our calculation for the relative energy as obtained by the DFT-based *ab initio* method[18] for three of the carbon families: the bucky-diamond, icosahedral, and fullerene structures at selected diameters ($d\leq 1.5$ nm). It can be seen that trends exhibited by the SCED-LCAO and DFT-based methods are consistent for the diameter-dependent relative energy, which lend further support to the conclusions drawn in this work for larger clusters based on the SCED-LCAO method.

B. Phase transformations

It has recently been reported in experiments that nanodiamond particles can transform into carbon onions by annealing.[10,24] Therefore, we have investigated in this work the effect of heating and slow cooling of a bucky-diamond C_{147} cluster. For this purpose, we perform a simulated annealing of the cluster based on the SCED-LCAO MD. This study revealed that depending on the manner of heating, one can obtain either onionlike or cage structures. For example, when the bucky-diamond C_{147} cluster is heated up to 2500 K and then slowly cooled to 0 K, one finds that the bonds connecting the diamond core to the fullerenelike surface are first broken, leading to an extension of the outer shell. Next, the inner diamond core becomes unstable and fragmented, and this eventually leads to the merging of these fragments into the exterior to form a double-shelled onionlike structure (top left of Fig. 4). The outer shell of this structure contains 119 atoms and the inner one contains 28 atoms. The results of our simulation are similar to the experimental observations reported in Refs. 10 and 25. We have conducted two other simulations. (i) One is heating the onionlike C_{147} cluster to 3200 K and subsequently cooling it to 0 K. In this simulation, bonds in the inner shell are broken and all the atoms in the interior move to the exterior, merging with the outer shell and thus forming a cagelike structure (middle right of Fig. 4). (ii) The other is gradually heating the bucky-diamond structure to 3500 K and then slowly cooling it to 0 K. In this case, the inner core is completely decomposed and all of the atoms in the interior have enough energy to move to the surface forming a cage structure (bottom of Fig. 4). We find that by slightly adjusting the thermostat, one can obtain different types of fullerenelike structures. We find that the total energy per atom decreases as one proceeds from the bucky-diamond phase to the onion phase and then to the cagelike phase, which is consistent with the energetics of carbon clusters shown in Fig. 3. Our studies for the transitions from a bucky-diamond/onionlike structure to a cagelike structure suggest a possible way to synthesize giant fullerenes.

Experimentally, phase transformations from onionlike structures to diamondlike structures have also been observed when carbon onions are heated to ~ 700 °C and irradiated with electrons.[25] Computer simulation studies corresponding to this reverse phase transformations may be feasible. As a first step toward this goal, we have studied the energetics of carbon onions corresponding to $C_{20}@C_{150}$, $C_{60}@C_{180}$, $C_{60}@C_{240}$, and $C_{80}@C_{320}$ with their diameters close to bucky-diamond clusters of either C_{147} or C_{275}. The results of this preliminary study are reported elsewhere.[26]

C. Highest occupied molecular orbital-lowest unoccupied molecular orbital gap of fullerenes

In this section we present our results for the size dependence of the highest occupied molecular orbital (HOMO)-lowest unoccupied molecular orbital (LUMO) gaps of the relaxed fullerene structures with diameters $d\leq 3.5$ nm. We find that the behavior of the HOMO-LUMO gaps as a function of the diameter of fullerenes is oscillatory with the gap ranging from 2 eV to 6 meV for the diameter range, as shown in Fig. 5. The magnitude of the energy gap oscillation appears to decrease as the size of the fullerene increases. This behavior is consistent with the expected property that the energy gap of a large fullerene must approach that of a graphene sheet. Furthermore, the pattern for the energy gap behavior found in the SCED-LCAO method is very similar to that obtained by our DFT-based electronic structure calculation using VASP.[18]
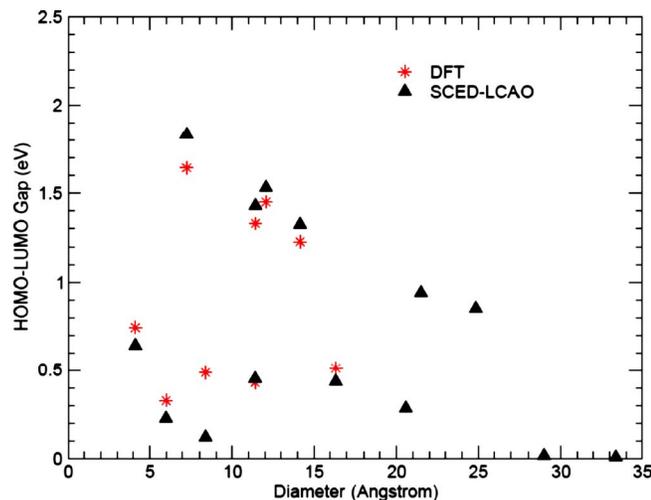
FIG. 5. (Color online) The diameter dependence of the HOMO-LUMO gaps for fullerenes as obtained by the SCED-LCAO and DFT calculations is shown.

IV. SUMMARY

In summary, we have conducted a comprehensive study of the energetics and relative stabilities of nanosized carbon clusters ($d \leq 5$ nm) that include bucky diamonds, icosahedral clusters, fullerenes, and fullerenelike structures (carbon cages and carbon onions) based on the SCED-LCAO MD. We have also studied the diameter dependence of relative energies of carbon clusters and the size dependence of the HOMO-LUMO gaps of fullerenes. The highlights of our findings are the following. (i) Among the known families of carbon clusters investigated, the fullerene family (with sp^2 bonding between its atoms) has the lowest energy for $d \leq 5$ nm. (ii) The relative energy ordering of the carbon structures studied is $E_{fullerene} < E_{onion} < E_{icosahedral} < E_{bucky-diamond} < E_{bulk-truncated}$ for $d \leq 5$ nm. (iii) Our estimation suggests that there may be a crossover at $d \sim 8$ nm in the relative energy values between bucky-diamond and icosahedral structures, making bucky-diamond structures more stable compared to icosahedral structures for $d > 8$ nm. (iv) Based on simulated annealing studies and depending on the heating and cooling scheme, we have identified three types of structural transformations for C_{147}: (a) the bucky-diamond structure to a double-shelled onion structure, (b) the double-shelled onion to a cage structure at elevated temperatures, and (c) a direct transformation from the bucky-diamond structure to a cage structure at even more elevated temperatures. The results provide a viable pathway for the synthesis of giant cage structures. It is conceivable that such giant fullerenelike structures may be used as molecular transporters for drug targeting. (v) The HOMO-LUMO gap as a function of the diameter of the fullerenes shows an oscillatory behavior that may be attributed to the symmetry of fullerenes with the gap oscillating between ~ 2 eV and 6 meV. The magnitude of the gap oscillations decreases as the size of the cluster increases in order to attain the zero gap of graphite at large diameters. In conclusion, we find that the interplay between the bonding nature, the size, and the symmetry of the cluster dictates the relative stability and structural and other properties of carbon clusters.

[1] H. W. Kroto, J. R. Heath, S. C. O'Brien, R. F. Curl, and R. E. Smalley, Nature (London) **318**, 162 (1985).
[2] R. Ettl, I. Chao, F. Diederich, and R. L. Whetten, Nature (London) **353**, 149 (1991).
[3] F. Diederich, R. Ettl, Y. Rubin, R. L. Whetten, R. Beck, M. Alvarez, S. Anz, D. Sensharma, F. Wudl, K. C. Khemani, and A. Koch, Science **252**, 548 (1991).
[4] B. L. Zhang, C. H. Xu, C. Z. Wang, C. T. Chan, and K. M. Ho, Phys. Rev. B **46**, 7333 (1992).
[5] G. Scuseria, Chem. Phys. Lett. **243**, 193 (1995).
[6] B. Dunalp and R. Zope, Chem. Phys. Lett. **451**, 422 (2006).
[7] D. Drabold, P. Ordejon, J. J. Dong, and R. M. Martin, Solid State Commun. **96**, 833 (1995); G. B. Adams, O. Sankey, J. B. Page, M. O'Keefe, and D. Drabold, Science **256**, 1792 (1992).
[8] L. Zeger and E. Kaxiras, Phys. Rev. Lett. **70**, 2920 (1993); L. Zeger and E. Kaxiras, Comput. Mater. Sci. **1**, 403 (1993).
[9] D. Ugarte, Carbon **33**, 989 (1995); D. Ugarte, Nature (London) **359**, 707 (1992).
[10] O. O. Mykhaylyk, Y. Solonin, D. Batchelder, and R. Brydson, J. Appl. Phys. **97**, 074302 (2005).
[11] J.-Y. Raty, G. Galli, C. Bostedt, T. W. van Buuren, and L. J. Terminello, Phys. Rev. Lett. **90**, 037401 (2003); J.-Y. Raty and G. Galli, Nature Mater. **2**, 792 (2003).
[12] Y. Zhao, Y.-H. Kim, M.-H. Du, and S. B. Zgang, Phys. Rev. Lett. **93**, 015502 (2004).
[13] L. Liu, C. S. Jayanthi, and S. Y. Wu, J. Appl. Phys. **90**, 4143 (2001).
[14] A. S. Barnard, S. P. Russo, and I. K. Snook, Phys. Rev. B **68**, 073406 (2003); A. S. Barnard, S. P. Russo, and I. K. Snook, J. Chem. Phys. **118**, 5094 (2003).
[15] M. Menon and K. R. Subbaswamy, Phys. Rev. B **49**, 13966 (1994).
[16] C. Leahy, M. Yu, C. S. Jayanthi, and S. Y. Wu, Phys. Rev. B **74**, 155408 (2006); S. Y. Wu, C. S. Jayanthi, C. Leahy, and M. Yu, in *Handbook of Materials Modeling*, edited by S. Yip (Springer, New York, 2005).
[17] C. S. Jayanthi, S. Y. Wu, J. Cocks, N. S. Luo, Z. L. Xie, M. Menon, and G. Yang, Phys. Rev. B **57**, 3799 (1998); S. Y. Wu and C. S. Jayanthi, Phys. Rep. **358**, 1 (2002).
[18] G. Kresse and J. Hafner, Phys. Rev. B **48**, 13115 (1993); G. Kresse and J. Furthmuller, *ibid.* **54**, 11169 (1996); G. Kresse and J. Furthnuller, Comput. Mater. Sci. **6**, 15 (1996).
[19] M. Menon and K. P. Subbaswamy, Phys. Rev. B **55**, 9231 (1997); M. Menon and K. P. Subbaswamy, *ibid.* **47**, 12754 (1993); M. Menon and K. P. Subbaswamy, *ibid.* **50**, 11577 (1994).
[20] J. E. Dennis, Jr. and R. B. Schnabel, *Numerical Methods for Unconstrained Optimization and Nonlinear Equation* (Society for Industrial & Applied Mathematics, Philadelphia, 1996).
[21] M. J. Frisch, G. W. Trucks, H. B. Schlegel *et al.*, GAUSSIAN03, Revision C.02, Gaussian, Inc., Wallingford, CT, 2004.
[22] C. Mailhiot and A. K. McMahan, Phys. Rev. B **44**, 11578 (1991).
[23] M. Yu *et al.*, Bull. Am. Phys. Soc. **51**, No. 1 (2006).
[24] V. L. Kuzentsov and Y. V. Butenko, in *Ultrananocrystalline Diamond Synthesis, Properties, and Applications*, edited by O. A. Shenderova and D. M. Gruen (William Andrew Publishing, New York, 2006), p. 405.
[25] F. Banhart and P. M. Ajayan, Nature (London) **382**, 433 (1996); F. Banhart, J. Appl. Phys. **81**, 3440 (1997).
[26] W. Q. Tian, M. Yu, C. Leahy, C. S. Jayanthi, and S. Y. Wu, J. Comput. Theor. Nanosci. **6**, 390 (2009).